Effects of Surface Temperature and Reynolds Number on Leeward Shuttle Heating

John J. Bertin*
The University of Texas, Austin, Texas
and
Winston D. Goodrich†
NASA Johnson Space Center, Houston, Texas

Heat-transfer data obtained at hypersonic shock tunnel conditions and three-dimensional flowfield computations were used to study the influence of surface temperature and Reynolds number on the heating experienced by the leeward fuselage area of the Space Shuttle Orbiter configuration. The basic results of this study indicate that systematic variations in the average total enthalpy within a boundary layer (as obtained through controlled nonadiabatic processes) have an influence on the heat transfer to downstream areas which can be correlated, even in three-dimensional separated flow areas. Specifically, the average separated-flow Stanton number for the fuselage leeward surface is shown to be moderately dependent on the windward-wall to freestream-total temperature ratio. Lowering the value of this ratio from ~0.4 (typical value for wind-tunnel tests) to ~0.1 (approximate value during flight at peak heating) reduces the average Stanton number by approximately 25%.

Nomenclature

h = local heat-transfer coefficient, defined in Eq. (2)
$h_{t,\mathrm{ref}}$ = heat-transfer coefficient for the reference stagnation-point heating rate
H = static enthalpy
H_t = stagnation enthalpy
L = axial model length, 0.3277 m (1.075 ft)
M_∞ = freestream Mach number
Pr = Prandtl number
$\dot{q}$ = local heat-transfer rate
$\dot{q}_{t,\mathrm{ref}}$ = heat-transfer rate to the stagnation point of an 0.305-cm (0.01-ft)-radius sphere (i.e., the reference radius reduced to model scale)
R = maximum body radius of the Apollo command module
r_{ref} = radius of a reference sphere reduced to model scale, 0.305 cm (0.01 ft)
Re_{nl} = Reynolds number behind a normal shock wave based on the wetted length from the stagnation point
Re_{ns} = Reynolds number behind a normal shock wave [see Eq. (1)]
$Re_{\infty,L}$ = freestream Reynolds number based on model length
s = wetted distance along a streamline
S = distance along the surface from the geometric center of the spherical heat shield of the Apollo command module
St = Stanton number [see Eq. (6)]
$\overline{St}_{\mathrm{scp}}$ = Stanton number averaged over those leeward gages in the "separated" region [see Eq. (7) and shaded area of Fig. 8 for A_{shaded}]
T_t = local static temperature
T_{lee} = leeward-surface temperature
T_r = recovery temperature
T_t = stagnation temperature
T_{wwd} = windward-surface temperature
u = streamwise velocity component
x = axial coordinate
y = coordinate measured normal to the model surface
α = angle of attack
δ = boundary-layer thickness
θ_H = enthalpy thickness [Eq. (4)]
μ = viscosity
ρ = density
ϕ = angular coordinate of the leeward gages, measured as a rotation about waterline $z400$

Subscripts

e = evaluated at the edge of the boundary layer
ns = evaluated behind a normal shock wave
w = evaluated at the wall
∞ = evaluated at the freestream conditions

Introduction

IN order to determine the convective heat-transfer distribution for the fuselage of the Space Shuttle Orbiter configuration, one must describe a three-dimensional flowfield that includes an extensive region of separated flow. Although the shear stress and the heat transfer in most of this region, which covers approximately 50% of the leeward fuselage area, are relatively low, locally high heating rates have been observed experimentally, e.g., by Hefner and Whitehead.[1,2] The flow mechanism of greatest importance to the surface environment in the separated region is the free-vortex layer. The effects of configuration geometry, angle of attack, Mach number, and Reynolds number on the generation of the vortices and their interaction with the leeward surface have been reviewed.[3] Preliminary scaling analyses, which consider the effects of surface temperature and Reynolds number of the leeward flowfield, indicate that, since much of the leeward surface area experiences relatively low heating rates, it would require little, if any, thermal protection material at flight conditions. Therefore, analyses and correlations that provide engineering predictions for the heating environment of the Orbiter leeward surface at flight conditions will aid in the design of a nonconservative, economical, reusable leeward surface structure and thermal protection system.

Received Jan. 5, 1976; presented as Paper 76-123 at the AIAA 14th Aerospace Sciences Meeting, Washington, D.C., Jan. 26-28, 1976; revision received April 9, 1976. This work was supported by the Johnson Space Center through NASA Contract NAS 9-13707.

Index categories: Jets, Wakes, and Viscid-Inviscid Flow Interactions; Boundary Layers and Convective Heat Transfer—Laminar.

*Associate Professor, Department of Aerospace Engineering and Engineering Mechanics. Member AIAA.

†Research Engineer, Structures and Mechanics Division. Member AIAA.

The motivation of this study was to verify experimentally the hypothesis that, under given flow conditions, a reduction in boundary-layer total enthalpy through heat transfer to cool surfaces can reduce substantially the total enthalpy of the fluid which is entrained in the downstream separated flow. Furthermore, if the local edge conditions remain constant, a reduction in separated flow total enthalpy should reduce separated flow heating. This hypothesis has analytical support in the work of Baum et al.[4] for two-dimensional configurations. However, because of the complexity of the Orbiter three-dimensional flowfield, an experimental investigation of this phenomenon was required. Correlations concerning the influence of local Reynolds numbers and boundary-layer cooling on the level of separated flow heating and on the production of attached vortical flows within separated flow regions also were sought during the investigation.

This paper presents the results of a recent experimental and analytical study designed to identify and correlate the pertinent flow parameters that affect the magnitude and distribution of the Orbiter leeward surface heating. This study supplements previous investigations on separated flow heating for the Orbiter by including a range of controlled temperature ratios (wall to total temperature), in addition to the more conventional parameters of Mach number and Reynolds number.

Experimental Program

The experimental program was conducted to investigate what effect the windward surface temperature has on heat transfer to the leeward surface of the Shuttle Orbiter.

Model

The model used in the test program was an 0.01-scale model of the Shuttle Orbiter configuration. The model did not include either the engine pods or the tail surface. A horizontal sheet of asbestos insulation ran the entire length of the model at waterline $z350$ and physically divided the model into two sections: the "windward" section and the "leeward" section. The model was designed so that the temperature of the windward surface could be varied from 233°K (420°R) to 800°K (1440°R), whereas the temperature of the leeward surface could be varied from 233°K (420°R) to 294°K(520°R). An Incaloy heater element was placed in the windward section during the runs where an elevated windward surface temperature was desired. For runs where the windward surface temperature was to be relatively cold, freon was passed through a cooling coil that replaced the heater element. For all runs, freon was passed through a cooling coil located in the leeward section.

The heat-transfer rates were determined from measurements of the transient surface temperature by means of thin-film resistance thermometers. An isometric sketch of the orbiter is presented in Fig. 1 to illustrate the locations of the 43 heat-transfer gages on the leeward surface. The locations of four gages, i.e., T8, T23, T29, and T37, are specified, since heat-transfer data for these gages will be presented in detail. For the present paper, the angular coordinate of a heat-transfer gage is defined by a rotation with respect to the x axis at the waterline $z400$. Thus, $\phi = 0°$ for the leeward pitch plane (which was also the plane of symmetry, since all tests were conducted at zero yaw and zero roll). The x axis along waterline $z338$ passes through the apex of the Orbiter. A horizontal plane passing through the $z338$ axis divided the windward surface from the leeward surface for the theoretical boundary-layer solutions (see Fig. 2).

Test Program

Heat-transfer rates were obtained in the Calspan 96-in. Hypersonic Shock Tunnel over a range of freestream Mach numbers from 10.0 to 18.6 and of freestream Reynolds numbers (based on model length) from 0.1×10^6 to 1.7×10^6. The data presented in the present paper were obtained at angle of attack of 30°. The values of the temperature ratio T_{wwd}/T_t used in the program were (nominally) 0.09, 0.18, and 0.31. The values of the ratio T_{wwd}/T_{lee} were (nominally) 1.00, 1.57, and 2.70. The values chosen for these parameters were intended to simulate, at one extreme, the temperature ratios obtained during atmospheric entry and, at the other extreme, values typical of those obtained in continuous-flow, supersonic wind tunnels. For additional details regarding the model, the test program, or additional data (such as the pressure measurements or other detailed heat-transfer correlations), the reader is referred to Ref. 5.

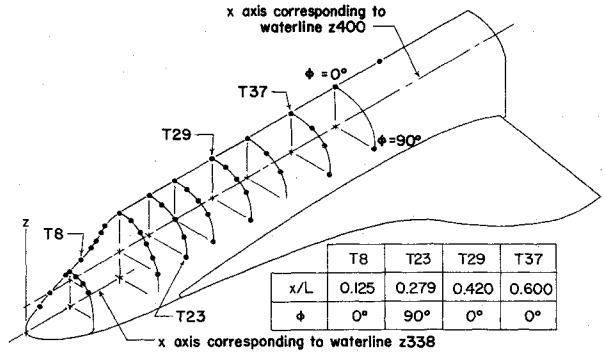

	T8	T23	T29	T37
x/L	0.125	0.279	0.420	0.600
ϕ	0°	90°	0°	0°

Fig. 1 Isometric sketch of the leeward heat-transfer gage locations.

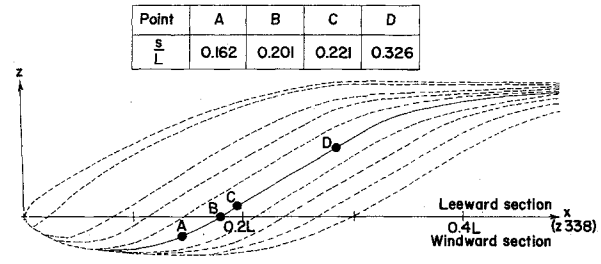

Point	A	B	C	D
$\frac{s}{L}$	0.162	0.201	0.221	0.326

Fig. 2 Sideview sketch of the Newtonian streamlines for the Orbiter (without a canopy).

Theoretical Solutions

Theoretical solutions for the viscous boundary layer of the Orbiter model at an angle of attack of 30° were generated to determine the effect of the test variables on the boundary layer prior to separation. The theoretical solutions for the nonsimilar, laminar boundary layer were computed using the code described in Ref. 6. Required as input for the code are the flow conditions at the edge of the boundary layer, the radius of the "equivalent" body of revolution, and the wall-temperature distribution.

The required inviscid solution‡ represents Newtonian flow over an Orbiter configuration whose geometry was essentially that of the model used in the present program except for the absence of the canopy. A sideview sketch of the Newtonian streamlines is presented in Fig. 2. The metric scale factor describing the streamline divergence was used to represent the radius of the equivalent body of revolution in the axisymmetric alalog for a three-dimensional boundary layer. The metric coefficients were calculated using the relations described by Rakich and Mateer.[8]

For the numerical solutions, the windward and the leeward sections were assumed to be isothermal, although not necessarily of equal temperature. A horizontal plane passing through the x axis (waterline $z338$) of Fig. 2 divided the windward section from the leeward section. For the solutions

‡This solution was provided by K. Houston of Lockheed Electronics Corporation (Houston) using the flowfield computational procedure presented in Ref. 7.

presented in this paper, the values of the windward surface temperature were as follows: case A, $T_{wwd}=0.090\ T_t$; case B, $T_{wwd}=0.176\ T_t$; and case C, $T_{wwd}=0.307\ T_t$. For all of the present cases, the leeward surface was $T_{lee}=0.114\ T_t$.

For the present paper, it was assumed that the fluid at the edge of the boundary layer had accelerated isentropically from a stagnation point behind a normal shock wave. In reality, neither the Newtonian pressure distribution nor the normal-shock-expansion assumption provides an accurate representation of the actual flowfield. However, the flow model is believed to be suitable, since the objective of these calculations is the determination of the effect of surface temperature on the correlation of leeward-surface heat-transfer rates, while holding local conditions constant. For additional details about the numerical algorithm and about the theoretical boundary-layer solutions, the reader is referred to Ref. 9 or 10.

The theoretical solutions presented in Figs. 3 and 4 were obtained along the streamline represented by the unbroken line of Fig. 2. This streamline was chosen since it encountered the free-vortex-layer separation downstream of the canopy but was upstream of the influence of the wing. Attention is called to the four points along the streamline which are of special interest:

1) The first, at $s=0.162L$, was just upstream of the rapid acceleration of the inviscid flow at the chine.

2) The second, at $s=0.201L$, was just upstream of the section interface. Thus, for these first two locations, the boundary layer has been subjected to a uniform temperature wall.

3) Since the third, at $s=0.221L$, is just downstream of the section interface, the solution at this location illustrates the effect of a sudden change in surface temperature.

4) The fourth, at $s=0.326L$, is just upstream of the "assumed" separation location. The term "assumed" is used, since, downstream of this location, the surface of the vehicle is inclined away from the freestream. However, the heat-transfer data indicate that the actual boundary layer remained attached downstream of this location.

For presentation in Fig. 3, the local heat-transfer rates have been divided by $\dot{q}_{t,\mathrm{ref}}$, which is the theoretical heat-transfer rate to the stagnation point of a 0.305-cm (0.01-ft)-radius sphere as calculated using the theory of Fay and Riddell.[11] The heat-transfer distributions are presented for a flow condition where $M_\infty=12.25$, $Re_{\infty,L}=0.59\times10^6$. For these freestream conditions, the Reynolds number behind a normal shock Re_{ns} was 536, where

$$Re_{ns}=\rho_{ns}u_{ns}r_{\mathrm{ref}}/\mu_{ns} \tag{1}$$

The characteristic dimension was that for a reference sphere reduced to model scale, i.e., $r_{\mathrm{ref}}=0.305$ cm (0.01 ft). Note that one of the present conclusions is that the parameters used in the correlations should be evaluated using a set of representative local properties downstream of the bow shock wave rather than the freestream conditions. Furthermore, Re_{ns} is a function both of the freestream Mach number and of the freestream Reynolds number. Thus, the leeward viscous flow is considered as characterized more by the Reynolds number behind a normal shock wave than by the freestream parameters. Consequently, correlations of the leeward-surface heat-transfer rates can be simplified by using a single, representative, local flow parameter rather than by using two freestream flow parameters.

At locations on the windward surface, e.g., points A and B of Fig. 2, the boundary layer increased by roughly 20% with temperature over the range of surface temperatures considered. Furthermore, at a higher wall temperature, the temperature gradient at the wall and, therefore, the heat-transfer rate were significantly less than the corresponding value for the lower wall temperature. At $s=0.201L$, the heat transfer for $T_{wwd}=0.307\ T_t$ (case C) was approximately 45% of the heat transfer for $T_{wwd}=0.090\ T_t$ (case A). The magnitude of

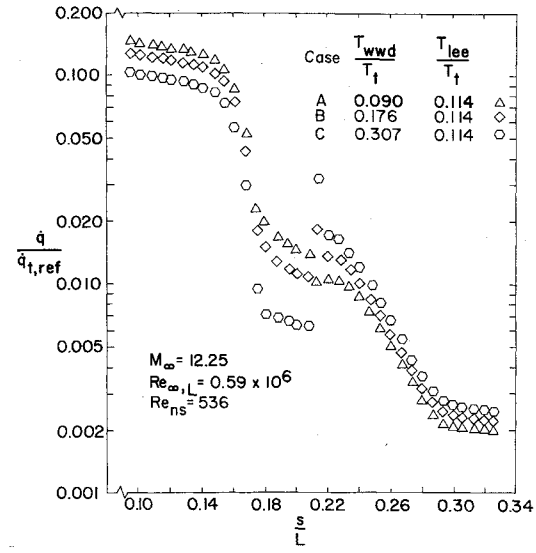

Fig. 3 The effect of the windward-section temperature on the streamwise heat-transfer distribution.

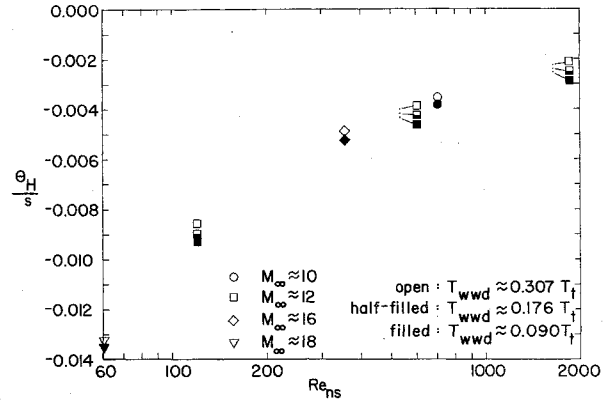

Fig. 4 Enthalpy thickness variation at the separation location with Reynolds number behind a normal shock wave.

the decrease was much greater than would be predicted using the relation

$$\dot{q}=h(T_r-T_w) \tag{2}$$

where

$$T_r=(Pr)^{1/2}(T_t-T_e)+T_e \tag{3}$$

Using this relation, the recovery temperature was approximately 0.86 T_t for all three cases. For this recovery temperature, (T_r-T_w) for case C was 72% of the value for (T_r-T_w) for case A. The decrease in (T_r-T_w) for the two cases was much less than the decrease in the computed heat-transfer rate. Thus, either the local heat-transfer coefficient or the recovery temperature (or both) depended on the surface temperature for this highly accelerated flow.

The leeward surface temperature was the same for all three cases, i.e., $T_{lee}=0.114\ T_t$. Thus, as the viscous flow passed from the windward section to the leeward section, it was subjected to an abrupt change in wall temperature. For cases B and C, the wall temperature decreased from windward values of 0.176 T_t and 0.307 T_t, respectively. However, for case A, the surface temperature increased slightly from the windward value of 0.090 T_t, as the viscous layer moved onto the leeward section. As noted previously, with the wall temperature at $s=0.201L$ equal to 0.307 T_t (i.e., case C), there was relatively little heat transferred from the viscous layer to the surface.

Thus, as the boundary layer passes onto the relatively cold, leeward section, there is a comparative "surplus" of energy available for heat transfer. This is reflected in the resultant increase in heat transfer evident in Fig. 3. A similar increase in heat transfer occurred for case B. As would be expected, the heat transfer for case A decreased abruptly as the boundary layer moved onto the leeward section. With all three viscous flows subjected to the same leeward surface temperature, the differences in the boundary-layer thickness for the three wall-temperature distributions quickly decreased. At the station just upstream of the separation location assumed for the theoretical solutions, i.e., $s=0.326\ L$, the boundary-layer thickness was essentially the same for all three cases. However, the average static temperature in the viscous layer was greatest for the flow that had been exposed to the hottest windward surface (i.e, $t_{wwd}=0.307\ T_t$ of case C). As a result, the computed heat transfer for case C was 1.13 times that for case B and 1.23 times that for case A. Thus, there was a reversal of the relative magnitude in the heat transfer for cases A, B, and C as the boundary layer encountered the step change in surface temperature at the interface. Since the amount of heat transferred from the boundary layer to the windward surface was related inversely to the windward surface temperature, the surplus of energy in the leeward boundary layer was related directly to T_{wwd}. As a result, the heat transferred from the attached, leeward boundary layer also was related directly to T_{wwd} (since the leeward surface temperature was the same for all three cases). As will be shown, this behavior in the theoretical heat-transfer rates at a position just upstream of boundary-layer separation is similar to the behavior of the experimental heat-transfer rates for gages located in the separated region itself.

The substantial differences that continued to exist in the temperature profiles downstream of the interface suggest the use of the enthalpy thickness to characterize the effect of the wall-temperature distribution on the boundary-layer solutions. The enthalpy thickness is defined as [12]

$$\theta_H=\int_0^{\delta}\frac{\rho\,u}{\rho_e u_e}\left(\frac{H}{H_e}-1\right)\mathrm{d}y \tag{4}$$

which, for a perfect gas, is

$$\theta_H=\int_0^{\delta}\frac{u}{u_e}\left(1-\frac{T_e}{T}\right)\mathrm{d}y \tag{5}$$

The enthalpy thickness is presented in Fig. 4 as a function of the Reynolds number behind a normal shock wave for flows, where

$$M_\infty=11.80,\quad Re_{\infty,L}=1.61\times10^6,\quad Re_{ns}=1644$$

$$M_\infty=12.25,\quad Re_{\infty,L}=0.59\times10^6,\quad Re_{ns}=536$$

$$M_\infty=11.68,\quad Re_{\infty,L}=0.12\times10^6,\quad Re_{ns}=120$$

$$M_\infty=15.70,\quad Re_{\infty,L}=0.61\times10^6,\quad Re_{ns}=357$$

$$M_\infty=10.10,\quad Re_{\infty,L}=0.54\times10^6,\quad Re_{ns}=705$$

$$M_\infty=18.59,\quad Re_{\infty,L}=0.14\times10^6,\quad Re_{ns}=61$$

Note that, for these wind-tunnel conditions, the enthalpy thickness can be corrected in terms of this single parameter Re_{ns} over the range of freestream Reynolds numbers and freestream Mach numbers considered. The enthalpy thickness was greatest, i.e., least negative, for those cases where the windward surface temperature was greatest, i.e., $T_{wwd}=0.307\ T_t$. Because the enthalpy thickness and the heat-transfer rate were greatest for the cases where the surface temperature of the windward section had been the greatest, one would expect the heat-transfer measurements for the downstream separated region to exhibit similar trends.

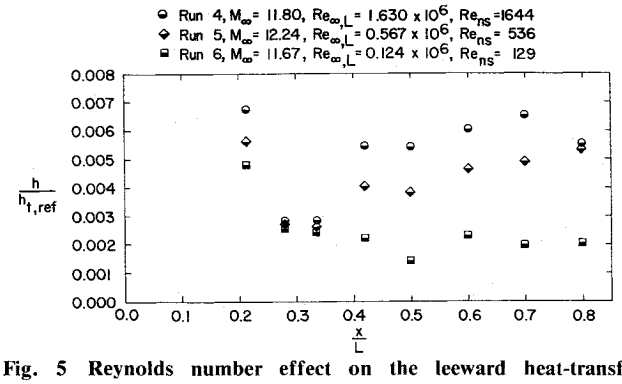

Fig. 5 Reynolds number effect on the leeward heat-transfer distribution.

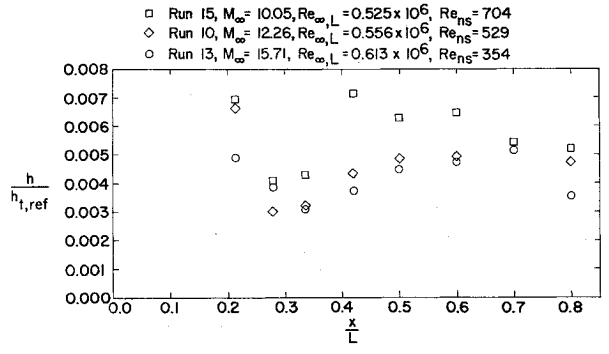

Fig. 6 Heat-transfer distribution in the leeward pitch plane for those runs with a nominal $Re_{\infty,L}$ of 0.6×10^6.

Experimental Data

The heat-transfer measurements for an angle of attack of 30° are presented either as 1) a dimensionless ratio of heat-transfer coefficients $h/h_{t,\mathrm{ref}}$, which involves the ratio of the measured, local heat-transfer rate to the theoretical heat-transfer rate to the stagnation point of a 0.305-cm (0.01-ft)-radius sphere as calculated using the theory of Fay and Riddell (for purposes of data presentation, the recovery factor r has been set equal to unity), or as 2) a Stanton number, where

$$St=\frac{\dot{q}}{\rho_\infty u_\infty(H_t-H_w)}=\frac{\dot{q}}{\rho_{ns}u_{ns}(H_t-H_w)} \tag{6}$$

Heat-Transfer Distributions for the Leeward Plane of Symmetry

The experimentally determined heat-transfer distributions for the gages located in the leeward pitch plane were similar to those observed during previous tests that were conducted in Tunnel B at Arnold Engineering Development Center (AEDC)[13] of a model with a protruding cockpit. A shock-induced increase in the heating rate was recorded at the gages located on the canopy windshield. The shock-perturbed, nondimensionalized value for the heat transfer was greatest for the highest Reynolds number. Although the nose-region geometry differed from the configurations tested in Tunnel B, the nondimensionalized heat-transfer coefficients for the windshield also increased with Reynolds number. The minimum heat transfer occurred just downstream of the canopy. Further downstream, the heat transfer was essentially constant at the lowest Reynolds number for the data of Fig. 5. Thus, the heat-transfer distribution indicated that the shear layer was laminar at the lowest Reynolds number. At the higher Reynolds numbers, the heat transfer increased markedly at $x\approx0.4L$ and remained high at the downstream

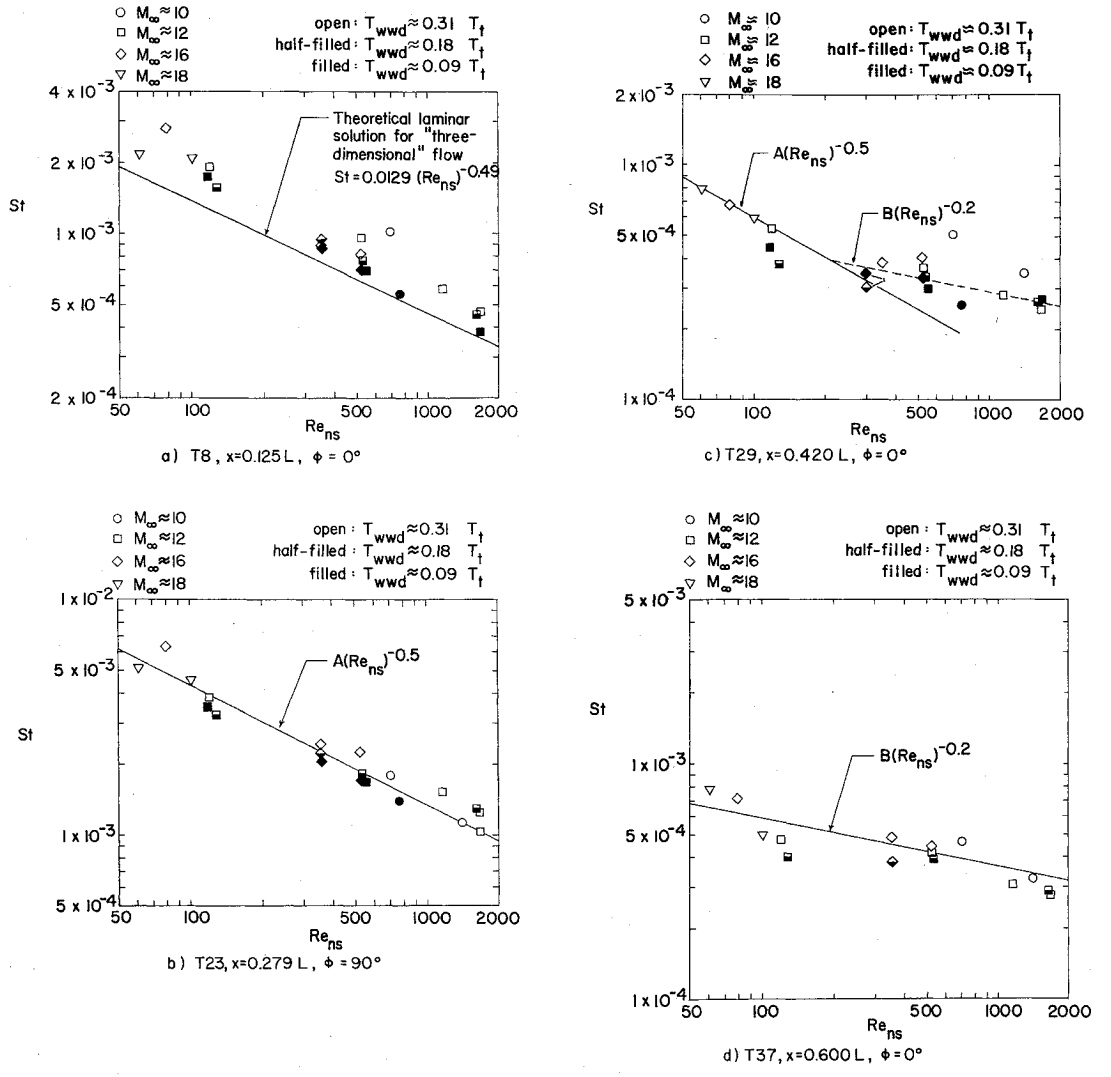

Fig. 7 Stanton number variation with Reynolds number behind a normal shock wave.

gages. This Reynolds-number-dependent behavior indicates that the increase was due to transition of the shear layer. A similar increase was evident in the heat-transfer distributions for all three Reynolds number of Ref. 13 ($1.6\times10^6 \le Re_{\infty,L} \le 7.8\times10^6$). Increased heating to the leeward surface due to transition of the shear layer also was reported by Zakkay et al.[14] and by Whitehead et al.[15] When the shear layer was turbulent, the dimensionless heat-transfer coefficient at a given station was Reynolds-number dependent. This Reynolds-number dependence resulted because the numerator contains the experimental value of the local heat transfer which resulted from a turbulent shear layer, whereas the denominator contains the theoretical laminar value. Since the Reynolds-number dependence for emerator differed from that for the denominator, the dimensionless ratio would not be expected to be independent of Reynolds number.

Locally high heating rates that were recorded at gages located on the lateral surface of the Orbiter indicated the occurren e of a viscous interaction between the vortex shed from the wing leading edge and the attached boundary layer on the fuselage. This viscous interaction also apparently affected the heat transfer in the separated region. Relatively high heat-transfer rates are evident in Fig. 5 for the gages downstream of $x=0.60L$ for the higher Reynolds numbers. Heat-transfer data reported by Zakkay et al.[14] also exhibited locally high, leeward heating rates near the aft end of the Orbiter (at $x\approx0.8L$). The mechanism responsible for the heat-transfer perturbation reported by Zakkay is believed to be comparable to that of the present tests.

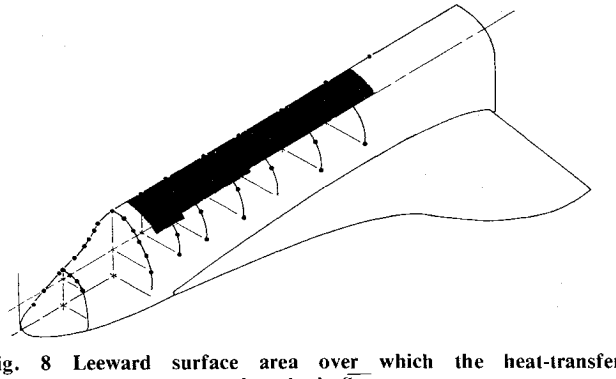

Fig. 8 Leeward surface area over which the heat-transfer measurements were averaged to obtain $\overline{St}_{sep}$.

The heat-transfer coefficients for those leeward pitch-plane gages downstream of the canopy are presented in Fig. 6 for runs where the freestream Reynolds number based on model length $Re_{\infty,L}$ was nominally 0.6×10^6. The controlled test parameter that was varied for these runs was the freestream Mach number. However, because the freestream Mach number varied, the Reynolds number behind a normal shock wave

$$Re_{ns} = \rho_{ns} u_{ns} r_{ref} / \mu_{ns}$$

also varied, as indicated in the legend of Fig. 6. Over the Mach number range of the present test program, Re_{ns} varied

by a factor of 2, even through $Re_{\infty,L}$ was approximately constant.

Thus, if one considers the leeward viscous flow as characterized more by the Reynolds number behind a normal shock wave than by the freestream Reynolds number, the nondimensionalized values of the heat-transfer coefficient increased with Re_{ns}. As noted, this is not unexpected, since the numerator would exhibit the Reynolds-number dependence of turbulent data, whereas the denominator would exhibit that for laminar theory. Thus, it is suggested that the data of Fig. 6 not be interpreted in terms of a Mach number effect but in terms of a Reynolds number effect. Furthermore, the parameters used in correlations of the data should be evaluated using properties downstream of the bow shock wave rather than the freestream conditions.

Heat-Transfer Data for Individual Gages

So that the relation between the local flow characteristics and the local heat transfer can be seen better, the experimental Stanton numbers (St) for a particular gage are presented in Fig. 7 as a function of Re_{ns}. The isometric sketch of Fig. 1 illustrates the locations of the gages for which heat-transfer data are presented. Data are presented for T8 (Fig. 7a), which is located in the nose region upstream of the canopy, T23 (Fig. 7b) which is located on the lateral surface where the boundary layer is attached, T29 (Fig 7c), which is located in the leeward pitch plane aft of the cockpit where the shear layer was transitional, and T37 (Fig. 7d), which is located in the leeward pitch plane aft of the cockpit where the shear layer was turbulent. Since the data are presented as a function of the Reynolds number behind a normal shock wave, the symbols are used to identify the nominal values for the other remaining test parameters.

a) A gage located on the nose upstream of the cockpit: Oil-flow patterns for the nose region of the Orbiter indicate the existence of a free vortex layer type of separation. An oil-flow pattern obtained using a partial model of the current Orbiter configuration exposed to a hypersonic flow ($M_\infty \approx 8$, $Re_{\infty/in} \approx 3 \times 10^6$ in Tunnel B of AEDC was presented in Ref. 9. At $x \approx 0.12L$, the circumferential component of the flow which initially was directed toward the leeward plane of symmetry reversed direction. At the separation line, oil accumulated and proceeded to travel down the separation line toward the rear of the Orbiter. The oil near the leeward plane of symmetry continued to flow from the attached region into the vortex region, indicating that the longitudinal component of the skin friction also was finite. The experimentally determined Stanton numbers for T8 are compared in Fig. 7a with the values for theoretical laminar solutions obtained using the code of Ref. 6. The local fluid properties at the edge of the boundary layer were evaluated assuming that the inviscid flow expanded isentropically from the stagnation point behind a normal shock wave in accordance with unpublished pressures measured at the Ames Research Center. The solutions for a "three-dimensional" boundary layer with small cross flow were generated using the axisymmetric analog. The metric scale-factor distribution that described the streamline divergence was computed from the Newtonian solutions provided by K. Houston of Lockheed Electronics Corporation. The theoretical solutions for three-dimensional flow underpredicted the heat transfer by (typically) one-third. Thus, the data indicate that, although the free-vortex separation of the boundary layer has occurred at this station away from the plane of symmetry, there was a strong axial flow component near the plane of symmetry, which was consistent with the oil-flow patterns discussed previously. Improved correlation between data and theory would be expected if the effect of the entropy gradients on the fluid properties at the edge of the boundary layer were to be included and if a metric-coefficient distribution based on the actual flowfield were to be used. Nevertheless, the similarity between the Reynolds-number dependence of the data and of the theoretical, laminar values indicated that the flow was laminar for the Reynolds numbers tested. Note also that the experimental heat-transfer rates were greatest for those runs where the windward-surface temperature was greatest ($T_{wwd} \approx 0.31\ T_t$). Thus, as discussed in the theoretical section, since there was less heat transferred from the boundary layer to the relatively hot windward surface, there as a "surplus" of energy available for heat transfer to the leeward section.

b) A gage located on the lateral surface of the fuselage where the boundary layer is attached: The experimentally determined Stanton numbers for gage T23 are presented in Fig. 7b. The location of this gage was close to that of point D in Fig. 2. However, because neither an experimental pressure distribution nor a realistic metric distribution was available, the theoretical solutions did not provide even rough estimates of the experimental values. However, the fact that the experimental values of the Stanton varied as $(Re_{ns})^{-0.5}$ indicates that the boundary layer in this region was laminar at all flow conditions. Furthermore, the experimental Stanton numbers were usually greatest for those runs where $T_{wwd} \approx 0.31\ T_t$. This was consistent with the correlation between the wall temperature and the theoretical laminar solutions presented in Fig. 3.

c) A gage located in the separated region downstream of the cockpit where the shear layer was transitional: The heat-transfer measurements for T29 are presented in Fig. 7c. The gage, which was located in the leeward pitch plane downstream of the canopy at $x = 0.420L$ (see Fig. 1), apparently was subjected to a vortical shear flow. This conclusion is based partly on the existence of a vortex-induced feather pattern along the lee meridan in the oil-flow pattern, which was obtained in a different program (presented in Ref. 9). For gage T29, the experimental Stanton numbers followed a laminar correlation $(Re_{ns})^{-0.5}$ for $Re_{ns} < 130$. For $Re_{ns} > 300$, the data followed a turbulent correlation, $(Re_{ns})^{-0.2}$. When the shear layer was laminar, the heat-transfer rates for T29 were roughly one-sixth of the values measured at a gage at the same station (i.e., $x = 0.420L$) on the side of the fuselage just upstream of separation. For $Re_{ns} > 300$, the heat-transfer rates for gage T29 were still significantly less than the values for the attached laminar boundary layer.

d) A gage located in the separated region downstream of the cockpit where the shear layer was turbulent: Heat-transfer measurements for gage T37 are presented in Fig. 7d. The experimentally determined Stanton numbers varied as $(Re_{ns})^{-0.2}$, the correlation for a turbulent shear layer. The highest heat-transfer rates recorded at T37 were those runs where $T_{wwd} \approx 0.31\ T_t$. (Unfortunately, the gage was inoperative for the runs where $T_{wwd} \approx 0.09\ T_t$.) Thus, although the shear layer was turbulent, the correlation between the local heating rate and the windward surface temperature is similar to that observed for gages where the shear layer was laminar. However, for two other gages in this region, there was no clear correlation between the local heat-transfer rate and the windward-surface temperature. The mixing due to the interaction with the vortical flow from the wing leading edge apparently eliminated the effect of the windward-surface temperature.

Averaged Stanton Numbers

The experimentally determined Stanton numbers were averaged for gages located in the "separated" region. The extent of the "separated" region, which is the shaded area in the isometric sketch of Fig. 8, was determined using the circumferential heat-transfer distributions. The average Stanton number was calculated using the expression

$$\overline{St}_{sep} = \Sigma \dot{q} \Delta A_{sep} / [\rho_{ns} u_{ns} (H_t - H_w) A_{shaded}] \qquad (7)$$

In evaluating $\Sigma \dot{q} \Delta A_{sep}$, it was assumed that the heat transfer measured at a particular gage acted uniformly over the rectangular surface element associated with the gage. The

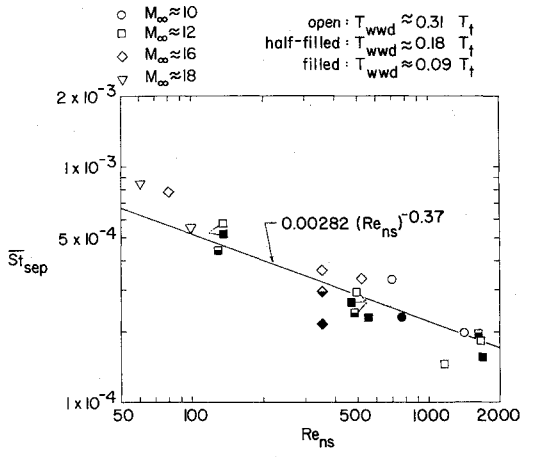

Fig. 9 Average Stanton number for the leeward "separated" region.

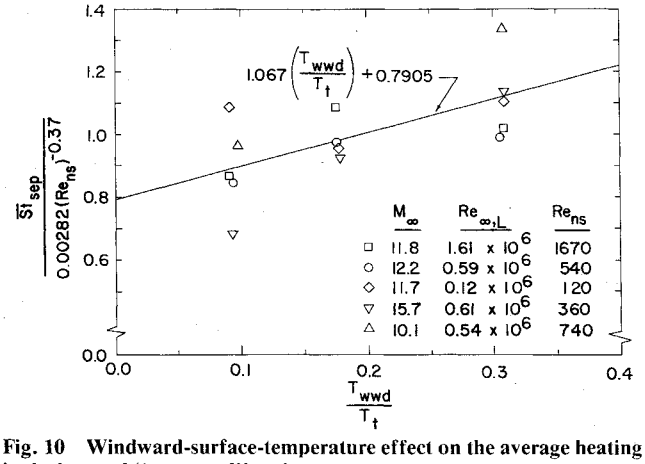

Fig. 10 Windward-surface-temperature effect on the average heating in the leeward "separated" region.

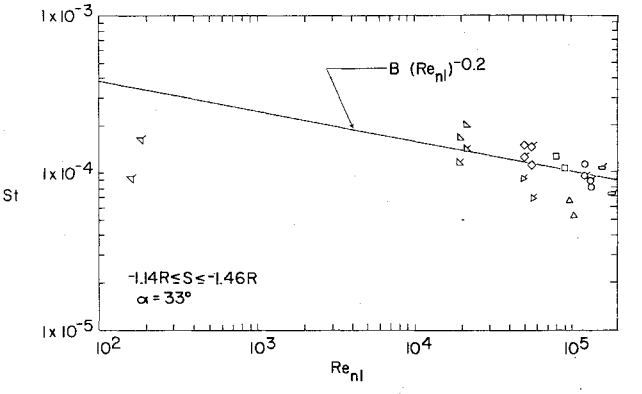

Fig. 11 Wind-tunnel heat-transfer data from the leeward pitch plane ($S < -1.5R$) of the Apollo configuration.

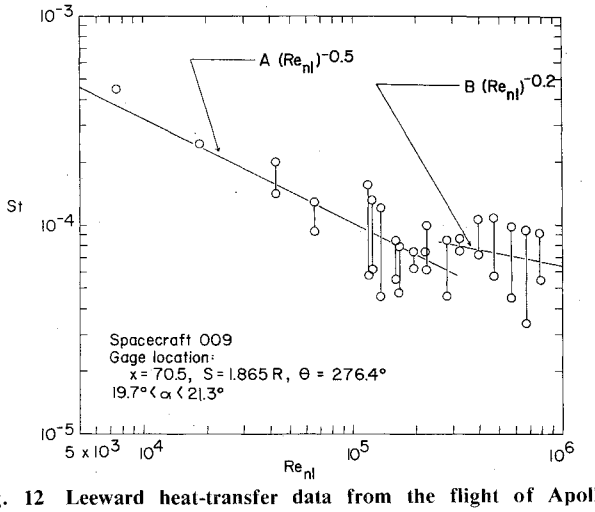

Fig. 12 Leeward heat-transfer data from the flight of Apollo spacecraft 009.

averaged values of the Stanton numbers for the gages in the separated region are presented in Fig. 9. Because of transition of the shear layer in the region of interest and the averaging of both laminar and turbulent heating rates, the data correlated as

$$\overline{St}_{sep} = 0.00282\ (Re_{ns})^{-0.37} \quad (8)$$

The correlation for the leeward Stanton number in Eq. (8) does not account for the effect that the windward-surface temperature had on the leeward heating. As noted when discussing the theoretical results and the heat-transfer measurements for individual gages, the leeward heat transfer was usually greatest when the windward-surface temperature was greatest. To obtain a measure of the wall-temperature effect, $\overline{St}_{sep}$ for a particular run has been divided by 0.00282 $(Re_{ns})^{-0.37}$ for that run and is presented in Fig. 10 as a function of T_{wwd}/T_t. As would be expected, the heat-transfer parameter increased as the temperature of the windward surface increased. If one assumes a linear correlation of the data, a least-squares fit yields the relation

$$\overline{St}_{sep}/0.00282\ (Re_{ns})^{-0.37} = 1.067(T_{wwd}/T_t) + 0.7905 \quad (9)$$

Thus, the experimentally determined Stanton numbers increased by approximately 26% over the range $0.09\ T_t < T_{wwd} < 0.31\ T_t$, i.e., the range for the present test program.

The Orbiter wind-tunnel data indicates the importance of shear-layer transition on the heat transfer to the leeward surface. Using the heat-transfer data for a particular gage, one can use correlations such as those of Fig. 7 to determine transition criteria for different positions on the vehicle. Note that Re_{ns} was calculated using the flow properties evaluated behind a normal shock wave and a single characteristic length regardless of the gage location. The values of Re_{ns} do not reflect the entropy gradients in the inviscid flow which would affect the value of the local flow properties or the length that would characterize the development of the viscous layer to the region of interest. In addition, significant differences may exist in the transition Reynolds numbers based on flight data and those based on wind-tunnel data. Such a difference in transition Reynolds numbers is exhibited in the Apollo data presented in Figs. 11 and 12.

Apollo wind-tunnel data[16] from AEDC Tunnel C and from the 4-ft Shock Tunnel of Calspan were re-examined. The Stanton numbers from the leeward pitch plane of the Command Module at an angle of attack of 33° are presented in Fig. 11 as a function of Re_{nl}, which is the Reynolds number based on flow properties behind a normal shock wave and the length from the stagnation point to the gage (as measured in the plane of symmetry). Stanton numbers are presented only for gages where the heat-transfer measurements were not affected by the presence of the sting. Heat-transfer measurements[17] from the flights of spacecraft 009 and spacecraft 011 also were re-examined. The Stanton numbers for a gage near the leeward plane of symmetry for 009 are presented in Fig. 12 as a function of Re_{nl}. Although the data are not presented herein, the data from the flight of spacecraft 011 were qualitatively similar to those of 009. The flight and the wind-tunnel Stanton numbers were in good agreement when the shear layer was turbulent. There were considerable differences between the flight and the wind-tunnel Stanton numbers when the shear layer was laminar. (The laminar

Stanton numbers for 011 were between the values of 009 and those from the wind tunnel.) The discrepancies that occurred when the shear layer was laminar are attributed to the differences in the angle of attack (i.e., 33° for the wind tunnel tests and approximately 20° for the flights) and to the considerable difficulties associated with measuring the very low heating rates experienced in flight during this time (i.e., Reynolds number range). However, the data indicate that the transition of the shear layer occurred at much higher Reynolds numbers in flight. The relatively low values in transition Reynolds number for the wind-tunnel tests may be due to transition-promoting phenomena peculiar to wind tunnels, such as noise.

Concluding Remarks

Based on the data and correlations obtained during this study, the following observations and conclusions can be made concerning the sensitivity of Orbiter-separated flow heating to the temperature ratio, the Mach number, and the Reynolds numbers:

1) Separated flow heating is reduced by nonadiabatic effects in upstream attached flows. The average separated flow Stanton number (or heat transfer) for the fuselage leeward surface is moderately dependent on the windward wall to total temperature ratio. Lowering the value of this ratio from ~ 0.4 (typical value for wind-tunnel tests) to ~0.1 (approximate value during flight at peak heating) reduces the average Stanton number by approximately 25%.

2) Representative "local" flowfield parameters improve correlation of separated flow heating data. Correlations of the separated flow Stanton number data should be made using a Reynolds number that uses properties evaluated downstream of the shock wave and, thus, incorporates the effects of both freestream Reynolds number and freestream Mach number.

3) If laminar flow can be maintained in flight, a reduction of approximately 50% can be achieved in separated flow heating. Stanton-number/Reynolds-number correlations indicate that much of the leeward fuselage flow experiences transition from laminar to turbulent flow in the wind tunnel when the Reynolds number behind a normal shock wave is 200. (This value occurs just before laminar peak heating during the Orbiter entry trajectory.) Comparisons of heat-transfer data from the leeward surface of the Apollo wind-tunnel programs indicate that, over a wide range of Reynolds number, the separated flow was laminar for the flight tests, whereas it was turbulent for the same value of Reynolds number for the wind-tunnel tests. Such differences could possibly be due to wind-tunnel phenomena, such as noise, which promote transition.

References

[1] Hefner, J. N. and Whitehead, A. H., Jr., "Lee Side Investigation, Part I – Experimental Lee-Side Heating Studies on a Delta-Wing Orbiter," *Space Shuttle Technology Conference, Vol I: Aerothermodynamics, Configurations, and Flight Mechanics*, NASA TM X-2272, April 1971.

[2] Hefner, J. N. and Whitehead, A. H., Jr., "Lee Side Flow Phenomena on Space Shuttle Configurations at Hypersonic Speeds, Part II – Studies of Lee-Surface Heating at Hypersonic Mach Numbers," *Space Shuttle Aerothermodynamics Technology Conference, Vol. II: Heating*, NASA TM X-2507, Feb. 1972.

[3] Dunavant, J. C., Narayan, K. Y., and Walberg, G. D., "A Study of Leeside Flow and Heat Transfer on Delta Planform Configurations," AIAA Paper 76-118, Washington, D.C., Jan. 1976.

[4] Baum, E., King, H. H., and Denison, M. R., "Recent Studies of the Laminar Base-Flow Region," *AIAA Journal*, Vol. 2, Sept. 1964, pp. 1527-1533.

[5] Mruk, G. K., Bertin, J. J., and Lamb, J. P., "Experimental and Theoretical Study of Shuttle Lee-Side Heat-Transfer Rates," Calspan Corp., Rept. ZC-5403-A-1, March 1975.

[6] Bertin, J. J. and Byrd, O. E., Jr., "The Analysis of a Nonsimilar Boundary Layer – A Computer Code (NONSIMBL)," The University of Texas, Austin, Texas, Aerospace Engineering Rept. 70002, Aug. 1970.

[7] Goodrich, W. D., Li, C. P., Houston, C. K., Meyers, R. M., and Olmedo, L., "Scaling of Orbiter Aerothermodynamic Data Through Numerical Flow Field Simulations," *Conference on Aerodynamics Analyses Requiring Advanced Computers*, Paper 50, NASA SP-347, Pt. II, 1975, pp. 1395-1410.

[8] Rakich, J. V. and Mateer, G. G., "Calculation of Metric Coefficients for Streamline Coordinates," *AIAA Journal*, Vol. 10, Nov. 1972, pp. 1538-1540.

[9] Bertin, J. J., Senalug, G., McBride, M., and Willman, R. B., "The Effect of Surface Temperature and Reynolds Number on the Leeward Heat-Transfer for a Shuttle Orbiter," The University of Texas, Austin, Texas, Aerospace Engineering Rept. 75002, April 1975.

[10] Bertin, J. J. and Goodrich, W. D., "Effects of Surface Temperature and Reynolds Number on Heat Transfer to the Shuttle Orbiter Leeward Fuselage," AIAA Paper 76-123, Washington, D.C., Jan. 1976.

[11] Fay, J. A. and Riddell, F. R., "Theory of Stagnation Point Heat Transfer in Dissociated Air," *Journal of the Aeronautical Sciences*, Vol. 25, Feb. 1958, pp. 73-85, 121.

[12] Schlichting, H., Chap. 15, *Boundary-Layer Theory*, McGraw-Hill, New York, 1960.

[13] Bertin, J. J., Faria, H. T., Goodrich, W. D., and Martindale, W. R., "Effect of Nose Geometry on the Aerothermodynamic Environment of Shuttle Entry Configurations," *Journal of Spacecraft and Rockets*, Vol. 11, May 1974, pp. 275-281.

[14] Zakkay, V., Miyazawa, M., and Wang, C. R., "Hypersonic Lee Surface Flow Phenomena Over a Space Shuttle," *Journal of Spacecraft and Rockets*, Vol. 12, Nov. 1975, pp. 667-673.

[15] Whitehead, A. H., Jr., Hefner, J. N., and Rao, D. M., "Lee-Surface Vortex Effects over Configurations in Hypersonic Flow," AIAA Paper 72-77, San Diego, Calif., Jan. 1972.

[16] Bertin, J. J., "Wind-Tunnel Heating Rates for the Apollo Spacecraft," NASA TMX-1033, Jan. 1965.

[17] Lee, D. B., Bertin, J. J., and Goodrich, W. D., "Heat-Transfer Rate and Pressure Measurements Obtained During Apollo Orbital Entries," NASA TND-6028, Oct. 1970.